Colloids and Surfaces B: Biointerfaces 190 (2020) 110947

Contents lists available at ScienceDirect

Colloids and Surfaces B: Biointerfaces

journal homepage: www.elsevier.com/locate/colsurfb

Toxicological profile of calcium carbonate nanoparticles for industrial applications

Marta d'Amora[a,*], Freddy Liendo[b], Fabio A. Deorsola[b], Samir Bensaid[b], Silvia Giordani[a,c,*]

[a] Nano Carbon Materials, Istituto Italiano di Tecnologia (IIT), via Livorno 60, 10144, Torino, Italy
[b] Department of Applied Science and Technology, Politecnico di Torino, Corso Duca degli Abruzzi 24, 10129, Torino, Italy
[c] School of Chemical Sciences, Dublin City University (DCU), Glasnevin, D09 C7F8, Dublin, Ireland

ARTICLE INFO

Keywords:
Calcium carbonate nanoparticles
Environment
Toxicity
In vitro
In vivo

ABSTRACT

Calcium carbonate nanoparticles ($CaCO_3$NPs) derived from CO_2 are promising materials for different industrial applications. It is imperative to understand their toxicological profile in biological systems as the human and environmental exposures to $CaCO_3$NPs increases with growing production. Here, we analyse the cytotoxicity of $CaCO_3$NPs synthesized from a CaO slurry on two cell lines, and *in vivo* on zebrafish (*Danio Rerio*). Our results demonstrate the $CaCO_3$NPs *in vitro* safety as they do not cause cell death or genotoxicity. Moreover, zebrafish treated with $CaCO_3$NPs develop without any abnormalities, confirming the safety and biocompatibility of this nanomaterial.

1. Introduction

Currently, the employment of several nanomaterials to improve the performances and the mechanical properties of the cement has gained considerable research interest [1,2]. Different nanoparticles, including titanium dioxide nanoparticles (TiO_2 NPs) [3], silica nanoparticles (SiO_2 NPs) [4], alumina nanoparticles (Al_2O_3 NPs) [5], and carbon nanotubes (CNTs) [6] have been included in cement-based materials, presenting potential benefits or limitations. In this framework, calcium carbonate nanoparticles ($CaCO_3$NPs) derived from CO_2 are currently being investigated as potential nanomaterials to be employed in these industrial applications [7,8], with the purpose of contributing to CO_2 capture and utilization directly in the industrial site in which CO_2 is available or produced [9,10]. In this regard, the cement industry is one of the major contributors to anthropogenic CO_2 emissions; therefore, the possibility to incorporate a CO_2-derived filler in the cement matrix is very attractive [10,11].

Calcium carbonate nanoparticles are believed to increase the strength of the cement, thanks to their unique properties, including a high surface area to volume ratio and high porosity. The $CaCO_3$ increases the kinetic of the C–S–H bonds formation since it acts as seeds for the hydration of the cement, which turns out to be accelerated by the $CaCO_3$. Thus the early age compressive and flexural strengths of the cement are increased [12–14]. Moreover, $CaCO_3$ increases the mechanical properties, because of their filling properties [13,14].

The extensive surge in the production and use of $CaCO_3$NPs, exposure for industry workers and the impact of their release, gives rise to an urgent need for a careful toxicological evaluation of these nanoparticles on ecosystems and humans. To address this issue, we evaluated the toxicity of $CaCO_3$NPs on two different cell lines: a mouse embryonic fibroblast cell line (NIH 3T3) and a human breast adenocarcinoma cell line (MCF7). The cytotoxic assessment was performed by the evaluation and estimation of viability, reactive oxygen species (ROS) generation and DNA damage under *in vitro* conditions and after treatment with different concentrations of $CaCO_3$NPs. Our results reported that $CaCO_3$NPs did not lead to an increase of cell death and reactive oxygen species or oxidative DNA damage, demonstrating their no cytotoxicity in both NIH 3T3 and MCF7 cells.

We further analyse the behavior of $CaCO_3$NPs on embryonic/larval zebrafish. Zebrafish are increasingly employed as models in high-throughput toxicological studies, to speed up the nanotoxicity assessment [15–17]. The value of these organisms relies on their genetic similarity with humans, small size and transparency [18,19]. We examined the growth and survival of embryos treated with different suspensions of $CaCO_3$NPs from 4 to 120 h post fertilization (hpf). $CaCO_3$NPs exposure produced no significant changes in the zebrafish biological parameters.

Our results demonstrated that calcium carbonate nanoparticles had no *in vitro* and *in vivo* toxic effect, reporting their high biocompatibility. Our study provides insights into the safety and healthy working environments in industries that use $CaCO_3$NPs derived from CO_2.

* Corresponding authors at: Nano Carbon Materials, Istituto Italiano di Tecnologia (IIT), via Livorno 60, 10144, Torino, Italy.
E-mail addresses: marta.damora@iit.it (M. d'Amora), silvia.giordani@dcu.ie (S. Giordani).

https://doi.org/10.1016/j.colsurfb.2020.110947
Received 16 October 2019; Received in revised form 19 February 2020; Accepted 4 March 2020
Available online 06 March 2020

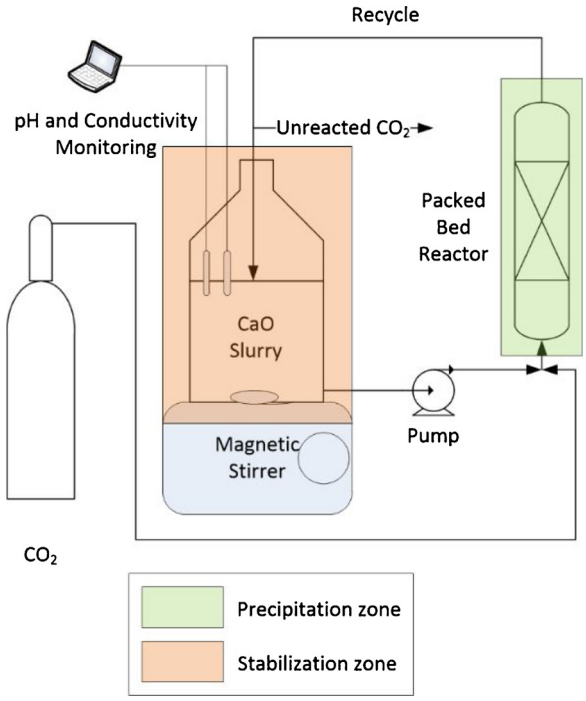

Fig. 1. Experimental setup for the synthesis of $CaCO_3$NPs.

2. Materials and methods

2.1. Synthesis of $CaCO_3$NPs

In the $CaCO_3$ synthesis, a slurry prepared with an analytical grade of CaO (Merck, purity ≥ 99 %) and deionized water, and CO_2 (purity: 99.9 %, supplied from SIAD, Italy) were employed. The $CaCO_3$NPs were synthesized through carbonation with pure CO_2 of a CaO slurry. The experimental setup consisted in semi-batch process employing a Packed Bed Reactor (PBR) filled with Raschig rings as random packing, shown in Fig. 1. The slurry is conveyed through a peristaltic pump into the PBR, where it gets in contact with the CO_2 and the precipitation takes place. The precipitated particles were immediately recirculated to the vessel, which is maintained at a constant stirring velocity. In such a way, two zones are individuated: i) the crystallization one, inside the PBR, ii) the stabilization one, inside the feed tank, where the pH is maintained high enough to provide a stable environment for the $CaCO_3$ particles, since under alkaline conditions growth and agglomeration phenomena of the CCnP are not favoured [20,21]. The CO_2 flow was stopped once the pH was less than 10.5, a value at which, according to the carbonate equilibria, the CO_3- formation is not favoured, thus reducing the $CaCO_3$ saturation (see Fig. 2). Then, once the process was finished, the synthesized particles were rapidly filtered by vacuum (pore size = 0.45 μm) and repeatedly washed with deionized water to eliminate ion excess. At last, the $CaCO_3$ powder was dried at 60 °C overnight and it was finally ready for characterization of their size, morphology and crystal phase. The parameters of the PBR are summarized in Table S1.

2.2. $CaCO_3$NPs characterization

Different characterization analysis were performed on the $CaCO_3$ powder. The dried powder was dispersed in isopropanol by means of ultrasonic mixing in order to obtain a stable crystal suspension (1 g L^{-1}) [22] and about 1 mL of sample was put into a disposable polystyrene cuvette and size and size distribution were measured by dynamic light scattering (DLS) method using particle size analyzer (Malvern nano ZS model). A 1 mL was also introduced into a zeta cell, and zeta potential values were measured by the Malvern Zetasizer.

The phase purity of the samples was examined by X-ray diffraction in the 2θ range of 20–70° with a scanning step of 0.013° and a radiation CuKα, k =1.54056 Å. The crystalline phase was identified by employing the Powder Diffraction File PDF-4/Minerals 2020 of JCPDS. Morphological characterization was obtained using Field Emission Scanning Electron microscopy (ZEISS MERLIN FE-SEM operated at 3 kV). The samples were prepared for electron microscopy observations by suspending a small amount of nanoparticles in isopropanol, through ultrasonic mixing for 30 min, subsequently by placing a drop of the dispersion on a copper grid coated with a layer of amorphous carbon, and finally the sample was dried at room temperature before FESEM analysis.

2.3. Cell culture

Mouse embryonic fibroblast cells (NIH 3T3) and human breast adenocarcinoma cells (MCF7) were grown in Dulbecco's modified Eagle's medium without phenol red (DMEM) (Life Technologies), supplemented with 10 % fetal bovine serum (FBS) (Life Technologies), 100 IU mL^{-1} penicillin and 100 μg mL^{-1} streptomycin (Life Technologies) at 37 °C in a humidified atmosphere containing 5 % CO_2.

2.4. Cell viability

NIH 3T3 and MCF7 cells were seeded at 1 × 10^4 cells/well in a 96 well plate and incubated overnight (o.n) in DMEM (37 °C, 5 % CO_2). On the next day, the medium was removed and the cells were treated with $CaCO_3$NPs at different concentrations (1, 5, 10, 25 and 50 μg/mL) in DMEM for 72 h. Cell viability was assessed using WST-1 assay (Roche Applied Science) as previously described [23,24].

2.5. Oxidative reactivity

Intracellular reactive oxygen species (ROS) generated by $CaCO_3$NPs were measured by using the 2′,7′-dichlorodihydrofluorescein diacetate (DCFH-DA) assay. A methanol DCFH-DA stock solution was diluted in DMEM without phenol red to obtain a 100 μM working solution. Cells were seeded in a 96 well plate and exposed to different concentrations of $CaCO_3$NPs for 2, 6 and 24 h. After the different time points, cells were rinsed three times with phosphate buffered saline (PBS, pH 7.4). 75 μL/well of DCFH-DA working solution was added to each well and plates were incubated a 37 °C for 30 min. PBS was used as a negative control, while hydrogen peroxide (H_2O_2) as a positive one. Subsequently, cells were rinsed with PBS and the fluorescent intensity was measured at 485/520 nm measured every 5 min over 30 min using a plate reader. ROS increase was calculated as the mean slope per min and normalized to the unexposed control. Each experiment was performed three times and the data are presented as mean values ± standard error of the mean of the replicates.

2.6. Comet assay

The levels of DNA damage in NIH 3T3 and MCF7 cells induced by $CaCO_3$NPs were measured by using the alkaline single-cell comet assay. Cells were seeded in 24 well and treated for 24 h with 1, 5, 10, 25 and 50 μg mL^{-1} of $CaCO_3$NPs for 6 and 24. PBS was used as a negative control, while H_2O_2 as a positive one. Cells were harvested, were rinsed twice in PBS and were trypsinized. The trypsin was inactivated by adding 1 mL of DMEM and the final suspension was by centrifugation (4 min at 18.000 × g, 4 °C). The cell suspension was mixed with low--melting agarose. 30 μl of aliquots were added on agarose-coated slides. Cells were lysed for 1 h on ice with lysis buffer. Next, they were placed in alkaline solution for 40 min followed by electrophoresis in the same buffer at 29 V for 30 min. Slides were neutralized, dried o.n. and fixed in methanol (5 min). The samples were stained with SYBR-green

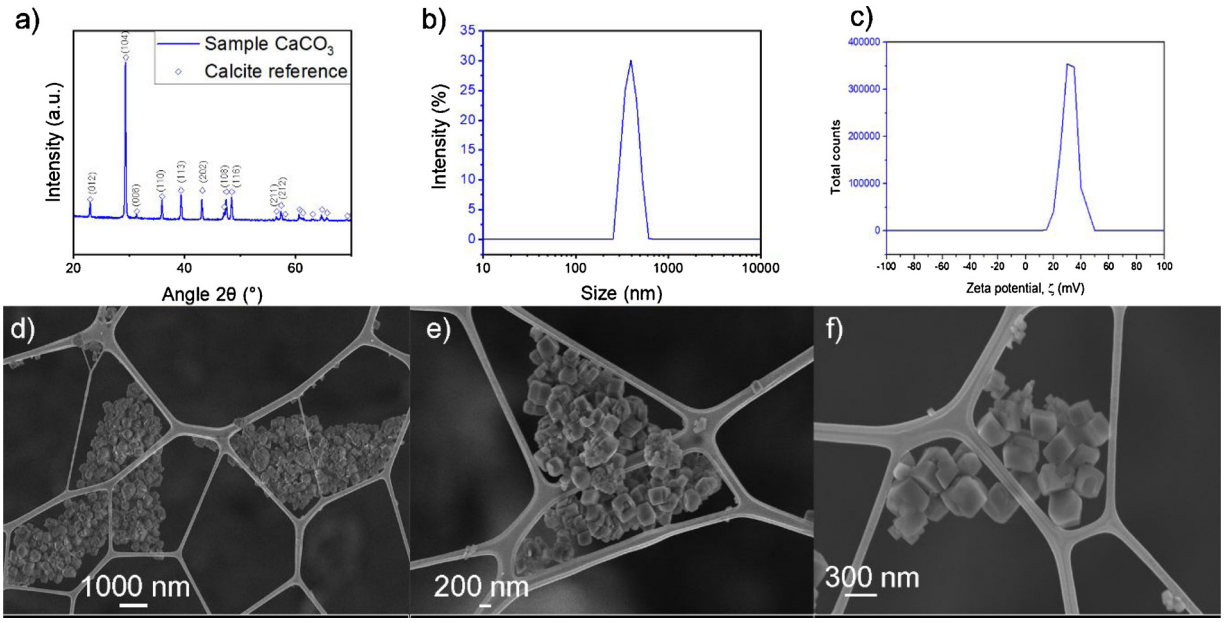

Fig. 2. $CaCO_3$NPs characterization. a) XRD spectra, b) CaCO3NPs size distribution, c) Zeta potential measurement, d-f) FE-SEM micrographs.

(Thermo Fisher Scientific, Waltham, MA) and scored by means of confocal microscopy (Nikon A1, Tokyo, Japan) with an automated image analysis system. At least 100 cells were analyzed per sample. Each experiment was performed three times. The extent of DNA damage was measured as the % DNA in the tail, which represents the fraction of the total DNA that is contained in the comet tail.

2.7. In vivo toxicity

Adult zebrafish (*Danio Rerio*) were kept and were spawned as previously described [25]. Embryos aged 4–5 hpf were collected, rinsed with E3 medium [26] and treated with 10, 50, 100 or 200 μg/mL of $CaCO_3$NPs until 120 hpf. Survival rate and hatching success were monitored every 24 h. The swimming and cardiac activities were noted at 72 hpf and the morphological changes at 96 hpf. Each experiment was performed three times. All animal experiments were performed in full compliance with the revised directive 2010/63/EU.

2.8. Statistical analysis

Results were expressed as mean ± standard deviations of three determinations. In the *in vitro* experiments, they were tested by one-way ANOVA or Student's t-test. Statistically, a significant difference was considered at $p < 0.05$. In the *in vivo* experiments, data were tested by one-way analysis of variance (ANOVA) in combination with Holm-Sidak post hoc to compare each treatment group with the negative controls. Statistically, a significant difference was considered at $p < 0.01$.

3. Results and discussion

3.1. Characterization of $CaCO_3$NPs

The synthesized $CaCO_3$ phase purity was characterized by XRD and compared to reference data and literature [27]. Fig. 2a shows the results from this analysis. The diffraction peaks are well consistent with pure calcite pattern, which is the most stable $CaCO_3$ crystalline phase [28–30]. No presence of other $CaCO_3$ crystalline phases, such as aragonite and vaterite, was determined. In fact, vaterite and aragonite phases could present some issues when employed as fillers, since they can solubilize and re-precipitate as calcite because of their greater instability. The sharpness of these peaks indicates the highly crystalline nature of the material. Fig. 2b shows a narrow size distribution (PSD), which is in a good agreement with the FESEM micrographs (Fig. 2d–f), where nanosized cubic calcite primary particles are seen. Zeta potential of −30 mV indicates that the particles are stable and do not agglomerate [20,21]. These particles have a cubic shape as seen in the FESEM micrographs (Fig. 2d–f), which is the classical morphology of calcite crystals [28,31]. Furthermore, this experimental setup provides CO_2 conversions equal to 18 %, which could mean a significant decrease in carbon footprint of the cement industry.

3.2. Toxicity evaluation

3.2.1. In vitro studies

3.2.1.1. Cellular viability. The cytotoxicity profile of $CaCO_3$NPs was determined in NIH 3T3 and MCF7 cells through WST1 cell metabolism-based assay to evaluate the mitochondrial activity for estimating cell proliferation and viability. The WST1 test estimates the cell metabolic activity *via* the reduction of salt to formazan and the amount of formazan is directly correlated to the number of metabolically active cells.

Different concentrations of $CaCO_3$NPs (1–50 μg mL^{-1}) were exposed to the two cell lines for 12, 24, 48, and 72 h. As shown in Fig. 3a, $CaCO_3$NPs did not enhance the WST1 reduction in the NIH 3T3 cells at different time points (Fig. 3a). Besides, the WST-1 did not form crystals with $CaCO_3$NPs in MCF7 cells was not affected by the presence of $CaCO_3$NPs (Fig. 3b). The evaluation of the WST-1 assays showed no cytotoxic effects of $CaCO_3$NPs at high concentrations (50 μg mL^{-1}) and long incubation time (72 h) in normal and cancer cells. Both cell lines were not susceptible to, $CaCO_3$NPs showing a significant cell viability increase for all the analyzed concentrations after 72 h and in some cases also after 48 (asterisks in Fig. 3a and b).

3.2.1.2. Oxidative reactivity. After a preliminary assessment of the potential harmful effects of $CaCO_3$NPs by cell viability on two different cell lines, we next evaluated their possible induction of intracellular oxidative stress and DNA damage. The ability of $CaCO_3$NPs to produce reactive oxygen species (ROS) was measured with the DCFH-DA assay. The experimental conditions were similar to the ones of cell viability studies. We exposed NIH 3T3 and MCF7 cells to different concentrations of $CaCO_3$NPs (1, 5, 10, 25 and 50 μg mL^{-1}) for

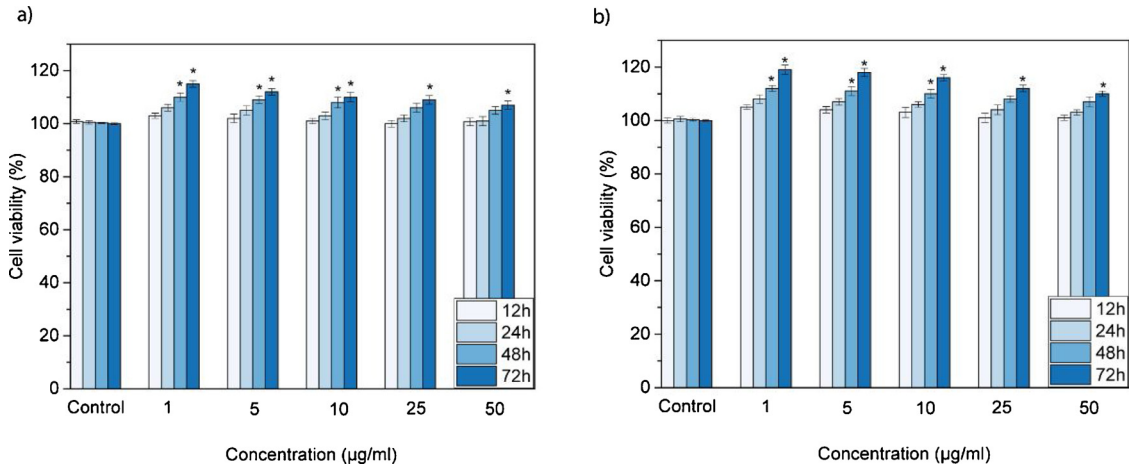

Fig. 3. (a) Cell viability of NIH 3T3 and (b) MCF7 cells treated with different concentrations (1, 5, 10, 25 and 50 μg mL^{-1}) of $CaCO_3$NPs for different times. Data are presented as the mean ± SD of three independent experiments (*p ≤ 0.05 in comparison to the control).

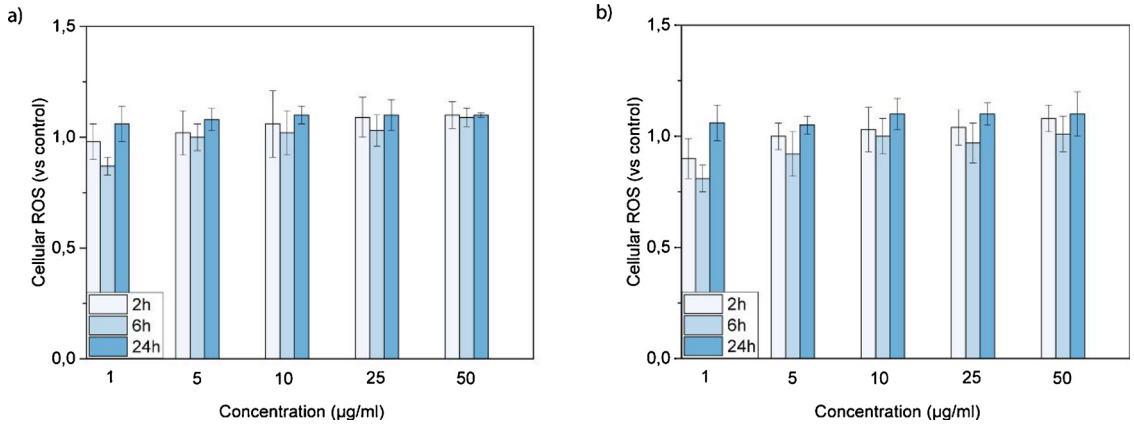

Fig. 4. (a) Intracellular ROS generation in (a) NIH 3T3 and (b) MCF7 cells treated with $CaCO_3$NPs revealed using the DCFH-DA assay. The ROS increase was calculated as the mean slope per min and normalized to the unexposed control. Data are represented as the mean ± SD of three independent experiments.

2, 6 and 24 h. None of the $CaCO_3$NPs doses caused any significant increase in the reactive oxygen species after the three different time points of exposure in NIH 3T3 (Fig. 4a) and MCF7 cells (Fig. 4b). These results indicated that $CaCO_3$NPs did not induce oxidative stress in both cell lines, confirming the non-cytotoxicity of this nanomaterial.

3.2.1.3. Genotoxicity. The level of DNA damage in NIH 3T3 and MCF7 cells induced by $CaCO_3$NPs was evaluated by using the comet assay. NIH 3T3 and MCF7 cells were treated with 1, 5, 10, 25 and 50 μg mL^{-1} of $CaCO_3$NPs for 6 and 24 h. As shown in Fig. 5, no DNA damage was induced at any concentration and time point in both cell lines. The tail intensities obtained for the different concentrations of $CaCO_3$NPs at 6 and 24 h were comparable with the values of the negative control samples. However, a significant difference with the controls was observed at the higher concentration of $CaCO_3$NPs. Cells showed again no toxic effects induced by $CaCO_3$NPs treatment.

3.2.2. In vivo studies

All the *in vitro* studies performed to assess the impact of $CaCO_3$NPs on cells have demonstrated the high cyto-biocompatibility of these particles. However, since the use of $CaCO_3$NPs will lead to human exposure, we complete their risk assessment in zebrafish during the development.

To evaluate the developmental toxicity of $CaCO_3$NPs, zebrafish embryos were treated with different concentrations of $CaCO_3$NPs (10, 50, 100 and 200 μg mL^{-1}). The survival rate, hatching success, swimming, and cardiac activities and morphological changes were analyzed during the early embryonic growth. $CaCO_3$NPs did not affect the survival rate (Fig. 6a), even if a significant difference ($p \leq 0.01$) was observed at 120 hpf, at higher concentration $CaCO_3$NPs (200 μg mL^{-1}). Correspondingly, the hatching success was not delayed or inhibited from the treatment with the different concentrations of $CaCO_3$NPs (Fig. 6b), presenting a significant difference only at 48 and 120 hpf at high concentration. Embryos hatched in their normal temporal window, between 48 and 72 hpf. The high values of survival and hatching rates revealed no significant toxic effects of $CaCO_3$NPs on these two biological parameters.

Moreover, the swimming and cardiac activities of larvae of 72 hpf were monitored. Exposure to $CaCO_3$NPs induced no significant effects on heartbeats. Spontaneous movements of treated larvae remained unchanged in comparison with the control group (see Fig. S1a and b in the Supplementary Material). These results confirmed that $CaCO_3$NPs did not cause zebrafish toxicity in the temporal window of investigation.

Other reports on nanomaterials that can be employed to improve the mechanical properties of the cement showed a perturbation in all these toxicological endpoints. In particular, silica NPs [32] and CNTs [33,34] induced a decrease in the survival rate or an increase in the mortality and a delay and strong inhibition in the hatching rate. Moreover, larvae treated with silica NPs presented an altered larval locomotor activity and bradycardia [35], while larvae exposed to CNTs had a significant reduction of the number of heartbeats [33].

Besides, the morphological changes in zebrafish groups treated with $CaCO_3$NPs were monitored at 96 hpf. The deformities produce by

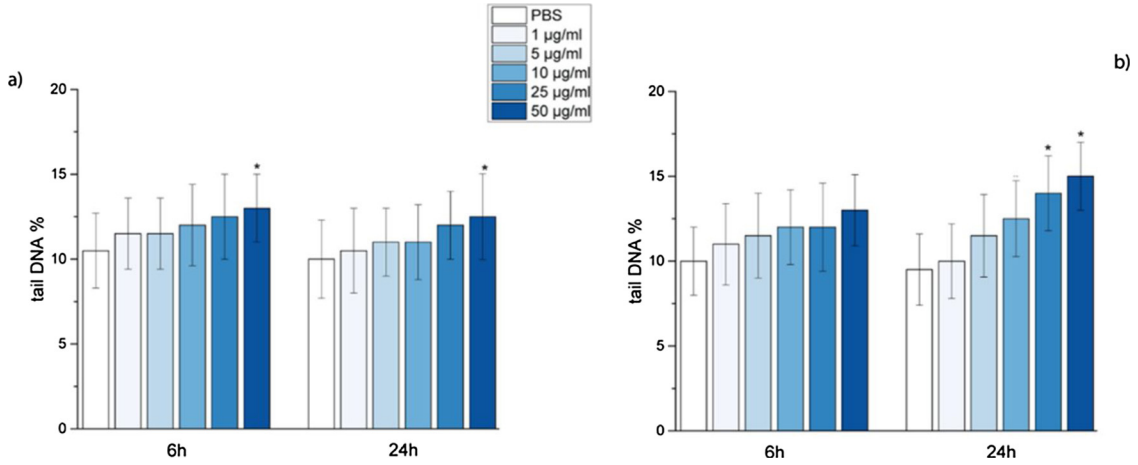

Fig. 5. Percent of DNA in the tail (tail DNA %) in (a) NIH 3T3 and (b) MCF7 cells. Data are represented as the mean ± SD of three independent experiments (*p ≤ 0.05 in comparison to the control).

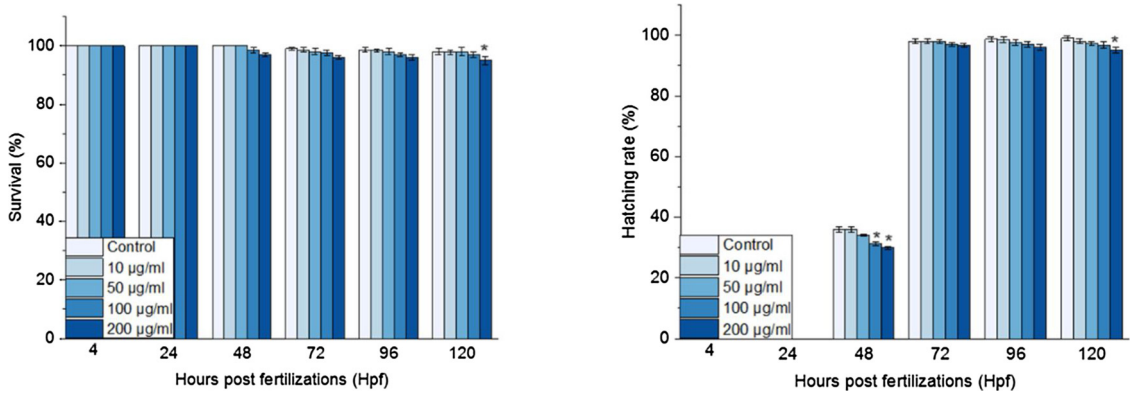

Fig. 6. Survival (a) and hatching rates (b) of zebrafish exposed to $CaCO_3$NPs. Data are presented as the mean ± SD of three independent experiments n = 80 (*p ≤ 0.01 in comparison to the control).

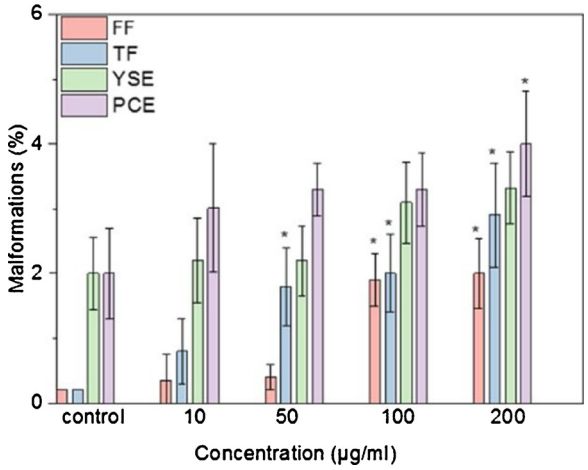

Fig. 7. Malformations of zebrafish induced by $CaCO_3$NPs. Data are presented as the mean ± SD of three independent experiments n = 80 (*p ≤ 0.01 in comparison to the control).

$CaCO_3$NPs, such as pericardial edema (PCE) and yolk sac edema (YSE), fin fold flexure (FF) and tail flexure (TF), were the most common induced by other classes of nanoparticles used as additives to the cement-based materials or other applications [32,36] (Fig. 7). As the concentration increases, the malformations percentages became higher. Even if significant differences between the phenotypes of samples of control and treated one was detected for some abnormalities and endpoints (asterisks in Fig. 7), the total percentage of malformations was still < 4 %, indicating the absence of toxic effects.

In conclusion, the zebrafish embryo/larvae screening showed that $CaCO_3$NPs are inert. These *in vivo* findings agreed with the previous *in vitro* results, confirming the complete safety of $CaCO_3$NPs produced from CO_2.

4. Conclusions

In the present study, we have reported on the fabrication of calcium carbonate nanoparticles from CO_2 and their toxicity assessments in cultured cells and more complex biological systems. We have shown that $CaCO_3$NPs can be easily and rapidly synthesized from a CaO slurry. Moreover, we have demonstrated that our $CaCO_3$NPs possess a high cyto-biocompatibility in normal and cancer cell lines. The cell viability presented high values and no cell death or increase in the levels of reactive oxygen species or DNA damage were detected on the two different cell lines. To gauge the safety of $CaCO_3$NPs with respect to human exposure, we investigated the specific interaction of the nanoparticles with zebrafish, as vertebrate models. We demonstrated the excellent biocompatibility of $CaCO_3$NPs in zebrafish during early development, reporting no mortality, inhibition of hatching, cardiac effects and no perturbation in the locomotor activity in embryos and larvae treated even at the higher concentration of nanoparticles evaluated. In conclusion, our work reported for the first time the complete biosafety of $CaCO_3$NPs derived from CO_2, suggesting that they can be employed as additives in the materials cement-based without any exposure risks on the environments and human health.

Author contributions section

M.d.A and S.G. conceived the idea and designed the experiments. F.L. performed the synthesis and characterization of $CaCO_3$NPs. M.d.A. performed all the biological experiments. F.A.D and S.B. supervised the synthesis and characterization of $CaCO_3$NPs. S.G. supervised the biological experiments. M.d.A. wrote the paper. S.G and S.B. contributed to revise the paper. All authors read and approved the final manuscript.

Funding

This project has received funding from the European Union's Horizon 2020 research and innovation program under grant agreement 768583– RECODE (Recycling carbon dioxide in the cement industry to produce added-value additives: a step towards a CO_2 circular economy) project.

Declaration of Competing Interest

The authors declare that they have no known competing financial interests or personal relationships that could have appeared to influence the work reported in this paper.

Appendix A. Supplementary data

Supplementary material related to this article can be found, in the online version, at doi:https://doi.org/10.1016/j.colsurfb.2020.110947.

References

[1] M. Tiong, R. Gholami, M. Rahman, Cement degradation in CO2 storage sites: a review on potential applications of nanomaterials, J. Pet. Explor. Prod. Technol. 9 (2018).
[2] S. Du, J. Wu, O. AlShareedah, X. Shi, Nanotechnology in cement-based materials: a review of durability, modeling, and advanced characterization, Nanomater. (Basel, Switzerland) 9 (2019) 1213.
[3] E. Mohseni, F. Naseri, R. Amjadi, M.M. Khotbehsara, M.M. Ranjbar, Microstructure and durability properties of cement mortars containing nano-TiO2 and rice husk ash, Constr. Build. Mater. 114 (2016) 656–664.
[4] T. Mendes, D. Hotza, W. Repette, Nanoparticles in cement based materials: a review, Rev. Adv. Mater. Sci. 40 (2015) 89–96.
[5] M. Heikal, M.N. Ismail, N.S. Ibrahim, Physico-mechanical, microstructure characteristics and fire resistance of cement pastes containing Al2O3 nano-particles, Constr. Build. Mater. 91 (2015) 232–242.
[6] O. Mendoza, W. PearlJr, M. Paiva, C. Miranda, R. Toledo Filho, Effect of a commercial dispersion of multi walled carbon nanotubes on the hydration of an oil well cementing paste, Front. Struct. Civ. Eng. 10 (2016) 174–179.
[7] Y. Boyjoo, V.K. Pareek, J. Liu, Synthesis of micro and nano-sized calcium carbonate particles and their applications, J. Mater. Chem. A 2 (2014) 14270–14288.
[8] R. Chang, D. Choi, M.H. Kim, Y. Park, Tuning crystal polymorphisms and structural investigation of precipitated calcium carbonates for CO2 mineralization, ACS Sustain. Chem. Eng. 5 (2017) 1659–1667.
[9] R. Chang, S. Kim, S. Lee, S. Choi, M. Kim, Y. Park, Calcium Carbonate Precipitation for CO2 Storage and Utilization: a review of the carbonate crystallization and polymorphism, Front. Energy Res. 5 (2017).
[10] L. McDonald, F.P. Glasser, M.S. Imbabi, a new, carbon-negative precipitated calcium carbonate admixture (pcc-a) for low carbon portland cements, Mater. Basel 12 (2019).
[11] I. Cosentino, L. Restuccia, G.A. Ferro, F. Liendo, F. Deorsola, S. Bensaid, Evaluation of the mechanical properties of cements with fillers derived from the CO2 reduction of cement plants, Procedia. Struct. Integr. 18 (2019) 472–483.
[12] I. Janotka, Hydration of the cement paste with Na2CO3 addition, Ceramics Silikaty 45 (2001) 16–23.
[13] S. Supit, F. Shaikh, Effect of Nano-CaCO3 on compressive strength development of high volume fly ash mortars and concretes, J. Adv. Concr. Technol. 12 (2014) 178–186.
[14] T. Matschei, B. Lothenbach, F. Glasser, The role of calcium carbonate in cement hydration, Cem. Concr. Res. 37 (2007) 551–558.
[15] M. d'Amora, S. Giordani, The utility of zebrafish as a model for screening developmental neurotoxicity, Front. Neurosci. 12 (2018) 976.
[16] K.A. Horzmann, J.L. Freeman, Making waves: new developments in toxicology with the zebrafish, Toxicol. Sci. 163 (2018) 5–12.
[17] Y.J. Dai, Y.F. Jia, N. Chen, W.P. Bian, Q.K. Li, Y.B. Ma, Y.L. Chen, D.S. Pei, Zebrafish as a model system to study toxicology, Environ. Toxicol. Chem. 33 (2014) 11–17.
[18] S. Saleem, R.R. Kannan, Zebrafish: an emerging real-time model system to study Alzheimer's disease and neurospecific drug discovery, Cell Death Discov. 4 (2018) 45.
[19] K. Howe, M.D. Clark, C.F. Torroja, J. Torrance, C. Berthelot, M. Muffato, J.E. Collins, S. Humphray, K. McLaren, L. Matthews, S. McLaren, I. Sealy, M. Caccamo, C. Churcher, C. Scott, J.C. Barrett, R. Koch, G.-J. Rauch, S. White, W. Chow, B. Kilian, L.T. Quintais, J.A. Guerra-Assunção, Y. Zhou, Y. Gu, J. Yen, J.-H. Vogel, T. Eyre, S. Redmond, R. Banerjee, J. Chi, B. Fu, E. Langley, S.F. Maguire, G.K. Laird, D. Lloyd, E. Kenyon, S. Donaldson, H. Sehra, J. Almeida-King, J. Loveland, S. Trevanion, M. Jones, M. Quail, D. Willey, A. Hunt, J. Burton, S. Sims, K. McLay, B. Plumb, J. Davis, C. Clee, K. Oliver, R. Clark, C. Riddle, D. Elliot, G. Threadgold, G. Harden, D. Ware, S. Begum, B. Mortimore, G. Kerry, P. Heath, B. Phillimore, A. Tracey, N. Corby, M. Dunn, C. Johnson, J. Wood, S. Clark, S. Pelan, G. Griffiths, M. Smith, R. Glithero, P. Howden, N. Barker, C. Lloyd, C. Stevens, J. Harley, K. Holt, G. Panagiotidis, J. Lovell, H. Beasley, C. Henderson, D. Gordon, K. Auger, D. Wright, J. Collins, C. Raisen, L. Dyer, K. Leung, L. Robertson, K. Ambridge, D. Leongamornlert, S. McGuire, R. Gilderthorp, C. Griffiths, D. Manthravadi, S. Nichol, G. Barker, S. Whitehead, M. Kay, J. Brown, C. Murnane, E. Gray, M. Humphries, N. Sycamore, D. Barker, D. Saunders, J. Wallis, A. Babbage, S. Hammond, M. Mashreghi-Mohammadi, L. Barr, S. Martin, P. Wray, A. Ellington, N. Matthews, M. Ellwood, R. Woodmansey, G. Clark, J.D. Cooper, A. Tromans, D. Grafham, C. Skuce, R. Pandian, R. Andrews, E. Harrison, A. Kimberley, J. Garnett, N. Fosker, R. Hall, P. Garner, D. Kelly, C. Bird, S. Palmer, I. Gehring, A. Berger, C.M. Dooley, Z. Ersan-Ürün, C. Eser, H. Geiger, M. Geisler, L. Karotki, A. Kirn, J. Konantz, M. Konantz, M. Oberländer, S. Rudolph-Geiger, M. Teucke, C. Lanz, G. Raddatz, K. Osoegawa, B. Zhu, A. Rapp, S. Widaa, C. Langford, F. Yang, S.C. Schuster, N.P. Carter, J. Harrow, Z. Ning, J. Herrero, S.M.J. Searle, A. Enright, R. Geisler, R.H.A. Plasterk, C. Lee, M. Westerfield, P.J. de Jong, L.I. Zon, J.H. Postlethwait, C. Nüsslein-Volhard, T.J.P. Hubbard, H. Roest Crollius, J. Rogers, D.L. Stemple, The zebrafish reference genome sequence and its relationship to the human genome, Nature 496 (2013) 498–503.
[20] S. Kilic, G. Toprak, E. Ozdemir, Stability of CaCO3 in Ca(OH)2 solution, Int. J. Miner. Process. 147 (2016) 1–9.
[21] E. Ulkeryildiz, S. Kilic, E. Ozdemir, Nano-CaCO3 synthesis by jet flow, Colloids Surf. Physicochem. Eng. Aspects 512 (2017) 34–40.
[22] V. Vergaro, E. Carata, E. Panzarini, F. Baldassare, L. Dini, G. Ciccarella, Synthesis of Calcium Carbonate Nanocrystals and Their Potential Application As Vessels for Drug Delivery, (2015).
[23] S. Lettieri, M. d'Amora, A. Camisasca, A. Diaspro, S. Giordani, Carbon nano-onions as fluorescent on/off modulated nanoprobes for diagnostics, Beilstein J. Nanotechnol. 8 (2017) 1878–1888.
[24] S. Lettieri, A. Camisasca, M. d'Amora, A. Diaspro, T. Uchida, Y. Nakajima, K. Yanagisawa, T. Maekawa, S. Giordani, Far-red fluorescent carbon nano-onions as a biocompatible platform for cellular imaging, RSC Adv. 7 (2017) 45676–45681.
[25] M. d'Amora, D. Cassano, S. Pocoví-Martínez, S. Giordani, V. Voliani, Biodistribution and biocompatibility of passion fruit-like nano-architectures in zebrafish, Nanotoxicology 12 (2018) 914–922.
[26] N. Nunn, M. d'Amora, N. Prabhakar, A.M. Panich, N. Froumin, M.D. Torelli, I. Vlasov, P. Reineck, B. Gibson, J.M. Rosenholm, S. Giordani, O. Shenderova, Fluorescent single-digit detonation nanodiamond for biomedical applications, Methods Appl. Fluoresc. 6 (2018) 035010.
[27] G.-T. Zhou, J.C. Yu, X.-C. Wang, L.-Z. Zhang, Sonochemical synthesis of aragonite-type calcium carbonate with different morphologies, New J. Chem. 28 (2004) 1027–1031.
[28] P.-C. Chen, C.Y. Tai, K.C. Lee, Morphology and growth rate of calcium carbonate crystals in a gas-liquid-solid reactive crystallizer, Chem. Eng. Sci. 52 (1997) 4171–4177.
[29] J. Kawano, N. Shimobayashi, A. Miyake, M. Kitamura, Precipitation diagram of calcium carbonate polymorphs: its construction and significance, J. Phys. Condens. Matter 21 (2009) 425102.
[30] J.D. Rodriguez-Blanco, S. Shaw, L.G. Benning, The kinetics and mechanisms of amorphous calcium carbonate (ACC) crystallization to calcite, viavaterite, Nanoscale 3 (2011) 265–271.
[31] A. Declet, E. Reyes, O. Suárez, Calcium carbonate precipitation: a review of the carbonate crystallization process and applications in bioinspired composites, Rev. Adv. Mater. Sci. 44 (2016) 87–107.
[32] J. Duan, Y. Yu, H. Shi, L. Tian, C. Guo, P. Huang, X. Zhou, S. Peng, Z. Sun, Toxic effects of silica nanoparticles on zebrafish embryos and larvae, PLoS One 8 (2013) e74606.
[33] X.T. Liu, X.Y. Mu, X.L. Wu, L.X. Meng, W.B. Guan, Y.Q. Ma, H. Sun, C.J. Wang, X.F. Li, Toxicity of multi-walled carbon nanotubes, graphene oxide, and reduced graphene oxide to zebrafish embryos, Biomed. Environ. Sci. 27 (2014) 676–683.
[34] H. Pan, Y.-J. Lin, M.-W. Li, H.-N. Chuang, C.-C. Chou, Aquatic toxicity assessment of single-walled carbon nanotubes using zebrafish embryos, J. Phys. Conf. Ser. 304 (2011) 012026.
[35] J. Duan, Y. Yu, Y. Li, Y. Li, H. Liu, L. Jing, M. Yang, J. Wang, C. Li, Z. Sun, Low-dose exposure of silica nanoparticles induces cardiac dysfunction via neutrophil-mediated inflammation and cardiac contraction in zebrafish embryos, Nanotoxicology 10 (2016) 575–585.
[36] M. D'Amora, A. Camisasca, S. Lettieri, S. Giordani, Toxicity assessment of carbon nanomaterials in zebrafish during development, Nanomaterials 7 (2017) 414.